Microscopic Characterization of Scalable Coherent Rydberg Superatoms

Johannes Zeiher,[1,*] Peter Schauß,[1] Sebastian Hild,[1] Tommaso Macrì,[2]
Immanuel Bloch,[1,3] and Christian Gross[1]

[1]*Max-Planck-Institut für Quantenoptik, 85748 Garching, Germany*
[2]*QSTAR, Largo Enrico Fermi 2, 50125 Firenze, Italy*
[3]*Ludwig-Maximilians-Universität, Fakultät für Physik, 80799 München, Germany*

(Received 6 March 2015; revised manuscript received 26 May 2015; published 12 August 2015)

Strong interactions can amplify quantum effects such that they become important on macroscopic scales. Controlling these coherently on a single-particle level is essential for the tailored preparation of strongly correlated quantum systems and opens up new prospects for quantum technologies. Rydberg atoms offer such strong interactions, which lead to extreme nonlinearities in laser-coupled atomic ensembles. As a result, multiple excitation of a micrometer-sized cloud can be blocked while the light-matter coupling becomes collectively enhanced. The resulting two-level system, often called a "superatom," is a valuable resource for quantum information, providing a collective qubit. Here, we report on the preparation of 2 orders of magnitude scalable superatoms utilizing the large interaction strength provided by Rydberg atoms combined with precise control of an ensemble of ultracold atoms in an optical lattice. The latter is achieved with sub-shot-noise precision by local manipulation of a two-dimensional Mott insulator. We microscopically confirm the superatom picture by *in situ* detection of the Rydberg excitations and observe the characteristic square-root scaling of the optical coupling with the number of atoms. Enabled by the full control over the atomic sample, including the motional degrees of freedom, we infer the overlap of the produced many-body state with a W state from the observed Rabi oscillations and deduce the presence of entanglement. Finally, we investigate the breakdown of the superatom picture when two Rydberg excitations are present in the system, which leads to dephasing and a loss of coherence.

DOI: 10.1103/PhysRevX.5.031015

Subject Areas: Atomic and Molecular Physics, Quantum Physics

Nonlinearities in light-matter coupling are usually weak, leading to a linear growth of the number of optical excitations with increasing photon flux. In contrast, the most extreme regime of strong nonlinearities is reached when an ensemble of many absorbers can host only a single excitation, such that one photon already saturates the medium. This can be realized with the aid of optical cavities [1] or, in free space, by atomic ensembles excited to Rydberg states [2]. For the latter, extremely strong dipolar interactions between Rydberg atoms block all but a single optical excitation in a volume of several cubic micrometers [3–6], effectively transforming the N atoms within this volume to one collective two-level system. Under uniform illumination, this "superatom" features enhanced coupling to the light field and the Rydberg excitation is symmetrically shared between the individual atoms [7]. The resulting singly excited Dicke state is also known as W state, whose many-body character is reflected in multipartite entanglement between its constituents [8]. Superatoms are valuable resources for quantum information. They have been proposed as collective qubits [4], and indeed, strong interactions between them were demonstrated recently [9]. These collective qubits have distinct advantages over single atoms that have previously been entangled using the strong Rydberg interactions [3,10–12]. First, the inherent collective enhancement of the atom-light coupling provides a single-photon interface and efficient entanglement transfer between atoms and light [13–15]. Second, the information is redundantly stored in the N constituent particles, protecting it against detrimental atom loss [16,17]. Further applications reach from advanced qubit encoding schemes in multilevel atoms [18,19] to multiatom gates [20,21]. Manipulation of the superatoms is at the heart of these proposals and amounts to controlling the strong and spatially dependent interactions of Rydberg atoms, which, in larger samples, lead to dephasing and prohibit the clear observation of Rabi oscillations [22–29]. However, for small systems of up to 16 atoms, Rabi oscillations have been directly observed [6,30–32], while for larger systems, indirect detection methods were required [33]. In all of these experiments, the spatial extension of the atomic sample in the propagation direction of the excitation light was non-negligible on the scale of

*johannes.zeiher@mpq.mpg.de

the wavelength and the motional degree of freedom of the atoms was not fully controlled. This leads to motional dephasing due to relative phases between the atoms fluctuating from shot to shot. This effect considerably complicates the characterization of the superatoms, leaving, for example, the demonstration of entanglement in larger samples as an open challenge.

In contrast, here we report on the preparation of isolated two-dimensional superatoms that are well described in the symmetric subspace. We control their shape locally on the single-atom level with submicrometer precision and their underlying atom number to better than shot noise. We detect the Rydberg excitations *in situ* with single-atom sensitivity and coherently manipulate collective systems with scalable size between 1 and 185 individual atoms. Together with the precise knowledge of the total atom number N in our experiments, this allowed for the direct confirmation of the predicted $\sqrt{N}$ enhancement of the Rabi coupling over 2 orders of magnitude. Additionally, the control of all quantum degrees of freedom, especially also the spatial ones, enables us to infer the presence of entanglement between the components of the superatom. Finally, we study the coherent breakdown of the superatom picture, recently investigated in the incoherent excitation regime [34]. We show that the breakdown occurs gradually in large samples and how multiple Rydberg excitations in the system lead to dephasing, which, however, can be reduced by postselection to the single-excitation subspace.

Our superatoms are formed out of an ensemble of ultracold atoms held in a two-dimensional optical lattice with unity occupation per lattice site [29]. This system is then approximately uniformly coupled to a Rydberg state with coupling strength Ω. The atoms occupy the Rydberg state only for a few microseconds, such that their motion in the optical lattice, typically on a millisecond time scale, can be safely neglected. The excited state is chosen such that for most of the experiments presented here, the system size is much smaller than the dipole blockade radius R_b. This dipole blockade originates from the van der Waals interaction, which causes an energy shift $\hbar\Delta_{\mathrm{vdW}} = C_6/R^6$ between Rydberg atoms separated by the distance R [4]. The extraordinary strong interaction tunes the excitation laser out of resonance up to the blockade distance $R_b = (C_6/\hbar\Omega)^{1/6}$ such that the system is restricted to a single Rydberg excitation. This single excitation is symmetrically shared among all N atoms if both coupling and interaction are effectively uniform. Hence, the system dynamics is confined to the symmetric subspace of zero ($n_e = 0$) and one ($n_e = 1$) excitations, whose basis states are the Fock states $|0\rangle = |g_1, \ldots, g_N\rangle$ and the entangled W state $|W\rangle = (1/\sqrt{N})\sum_{i=1}^{N} |g_1, \ldots, r_i, \ldots, g_N\rangle$, where g_i and r_i label the ith atom in the ground or Rydberg state. Then, the Hamiltonian can be written in the simple form $H = \hbar\sqrt{N}\Omega/2(|0\rangle\langle W| + |W\rangle\langle 0|)$, where the symmetry-induced collectively enhanced coupling $\sqrt{N}\Omega$ appears explicitly. The collective Bloch sphere [Fig. 1(a)] offers a convenient way of representing states within the symmetric subspace via their Husimi quasiprobability distribution [35,36]. The state $|0\rangle$ lies at the south pole of the sphere, while $|W\rangle$ corresponds to a ringlike structure. These many-body states form the basis for the superatom.

For the preparation of the superatoms, our experiment starts with a two-dimensional degenerate gas of rubidium 87 in the $|F = 2, m_F = 2\rangle$ hyperfine state, confined in a single antinode of a vertical (z-axis) optical lattice at a lattice depth of $80E_r$. Here, E_r is the lattice recoil energy of our square lattice with periodicity $a_{\mathrm{lat}} = 532$ nm. We prepare a unity filling Mott insulator of approximately 200–500 atoms by adiabatically switching on two orthogonal lattices in the $x - y$ plane to $40E_r$. We then use our local addressing technique to precisely control the size and shape of the atomic sample to a square with diagonal length D containing between 1 and 185 atoms with an average filling 0.87(5) [37,38]. This ensures that the edges and the total atom number of the atomic samples are well defined, allowing us to measure total atom-number fluctuations up to 4 dB below shot noise [Figs. 1(b) and 1(c)]. The atoms are then coupled to the $68S_{1/2}, |m_J = -1/2\rangle$ Rydberg state via a two-photon scheme (red laser with wavelength 780 nm and blue laser with wavelength 480 nm) [29]. The excitation beams are counterpropagating perpendicular to the atomic plane (z direction) with waists $w_0 = 44(2)$ μm for the red and $w_0 = 17(5)$ μm for the blue beam. The van der Waals coefficient of the $68S$ state is $C_6 = h\,630\ \mathrm{GHz}\,\mu\mathrm{m}^6$, resulting in a blockade radius of $R_b = 11.7(1)$ μm for the single-particle Rabi frequency of $\Omega = 2\pi \times 240(30)$ kHz. We detect the Rydberg atoms *in situ* using an efficient ($> 99.9\%$) pushout of the ground-state atoms lasting 8 μs followed by a stimulated depumping of the Rydberg atoms back to the ground state. The remaining atoms are then imaged using *in situ* fluorescence detection with a position resolution of approximately ± 1 lattice site [29]. From our data, we infer an overall efficiency of $\eta = 0.67(5)$ for the spatially resolved detection of a single Rydberg atom. The spatial control over the sample allows for microscopic control of the superatom size. As long as we ensure $R_b \gg D$ (up to and including 131 atoms), we observe coherent enhanced Rabi oscillations between the zero- and one-excitation subspaces. Here, the ratio of the amplitude of the Rabi oscillations to the total atom number scales as $1/N$ as opposed to being constant for independently oscillating particles. In Fig. 1(d), we illustrate this scaling for two exemplary cases of 8 and 131 atoms.

In order to characterize the prepared superatoms microscopically, we measure the spatial distribution of the observed Rydberg atom and the excitation statistics during the Rabi oscillation (Fig. 2). For different sample sizes between 1 and 185 atoms, we drive Rabi oscillations by

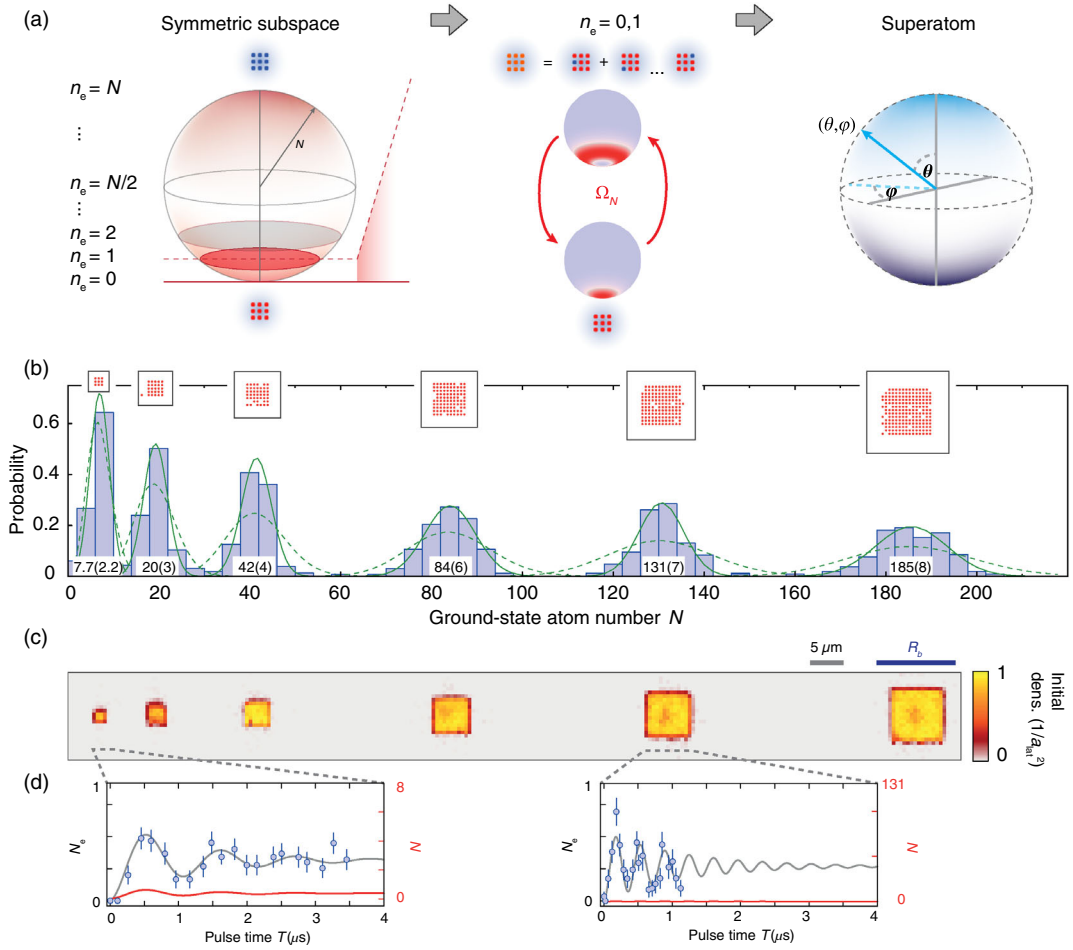

FIG. 1. Superatom preparation. (a) Illustration of the symmetric ground and singly excited state (W state). Left: N-atom collective Bloch sphere with its basis states (labeled by excitation numbers n_e) and coupled states highlighted [south pole ($n_e = 0$) and singly excited state ($n_e = 1$), represented by the red plane]. The small pictograms above and below the sphere depict the lattice system with atoms in the ground (red) and Rydberg (blue) states. The dashed red line indicates a zoom into the subspace spanned by the lowest two states. The Husimi distribution of these states and their enhanced coupling Ω_N is shown in the center. This accessible state space defines a superatom represented by the standard Bloch sphere on the right. (b) Atom-number histograms of the initially prepared samples (blue bars) with Gaussian fits (solid green line). The numbers give the mean and standard deviation for each data set. Measured and reconstructed occupation of lattice for exemplary initial states is depicted above the respective histograms; see the schematic pictograms in (a). The Poissonian distribution with the same mean atom number is shown as a reference (dashed green line). (c) Averaged initial ground-state atom distributions for the respective histograms above. The size of blockade radius R_b is shown by the blue bar. (d) Rabi oscillation data (blue points) and sinusoidal fits with exponentially decaying contrast (solid gray line) for $N = 7.7(2.2)$ and $N = 131(7)$. The red line shows the same fit on an axis scaled to the number of ground-state atoms N (right axis). All error bars denote the standard error of the mean (s.e.m.).

illuminating the sample with the coupling lasers for varying duration T. For each T, we repeat the experiment 25–30 times and extract the mean Rydberg number N_e [Fig. 2(a)]. The dramatic acceleration of the Rabi oscillation with N is clearly visible in the data. Additionally, we compare the spatial distribution of the Rydberg atoms (integrated over all T) to the initial distribution of ground-state atoms. Within statistical uncertainty, we find a flat distribution consistent with the uniform coupling assumption [Fig. 2(b)]. We experimentally confirm the picture of a fully dipole blockaded sample by extracting the histogram of the Rydberg excitation numbers n_e both integrated over the whole observation time T and as well at the π-pulse time T_π. For sample sizes up to 131 atoms, the probability of measuring doubly excited states with two detected Rydberg atoms is below 1%. We obtain typically 1–4 images with two excitations per 500–800 shots. This is compatible with the expected number of falsely detected Rydberg atoms due to imperfect removal of ground-state atoms in the detection process [29]. For the largest sample used in our experiments, the blockade starts to break down and the probability to detect two Rydberg atoms increases to 4.8(1.0)% (27 events per 564 shots). None of the data shown here are corrected for the detection efficiency, and the

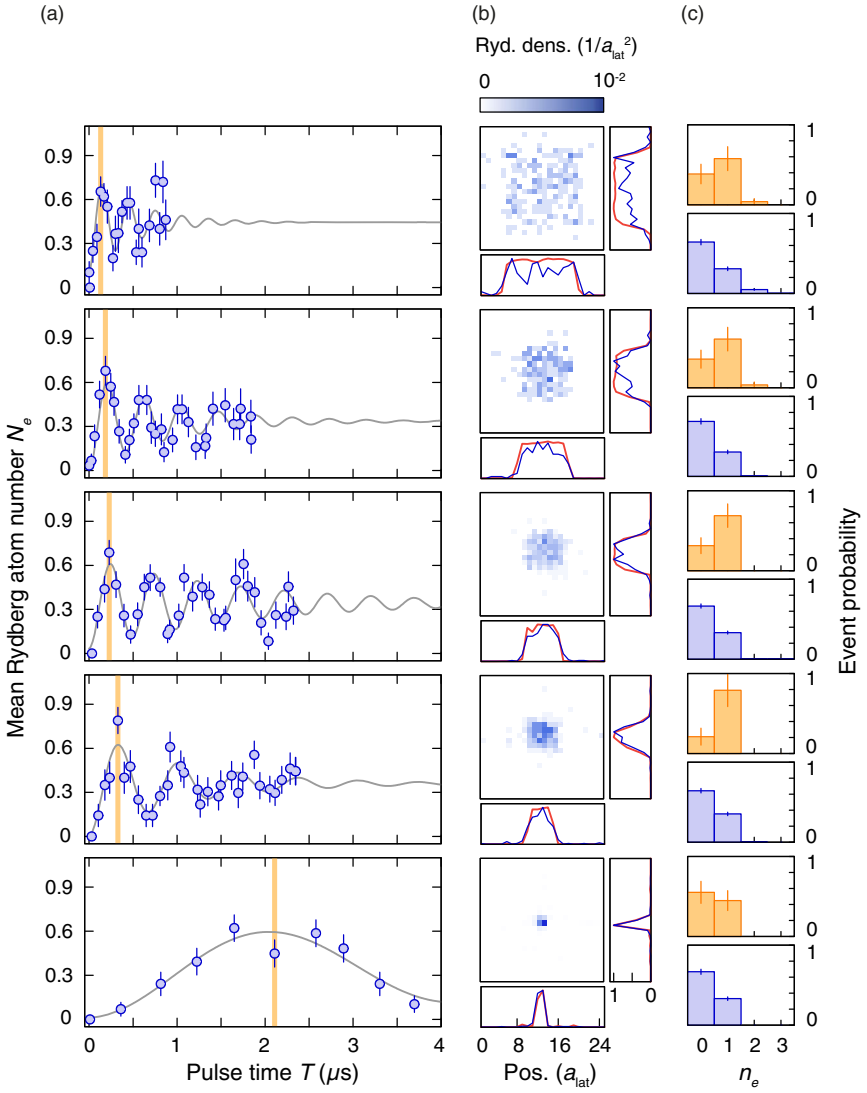

FIG. 2. Collective Rabi oscillations. (a) Collective Rabi oscillation data of the mean Rydberg atom number N_e (blue points) for different numbers of ground-state atoms $N = 185(8)$, 84(6), 42(4), 20(3), 0.74(0.60) (top to bottom) with exponentially decaying sinusoidal fits (gray). All error bars are s.e.m. (b) Density of detected Rydberg atoms for the data sets in (a) with normalized vertically or horizontally averaged density (solid blue line) compared to the initial state atom distributions (solid red line). (c) Histograms of the Rydberg excitation number integrated over the total oscillation (blue bars) and at the position of the first maximum [orange bars, position in (a) marked by solid orange line].

measured excitation number after T_π is consistent with $N_e = 1$ when taking it into account.

One striking signature of the superatom is its symmetry-enhanced coupling to the radiation field. We extract the oscillation frequency Ω_N, the decay time τ, and a global offset A from the data shown in Figs. 1(d) and 2(a) via a fit to $N_e = \eta[A - e^{-t/\tau}\cos(\Omega_N t)/2]$. Indeed, we confirm the expected scaling $\Omega_N \propto \sqrt{N}$ over 2 orders of magnitude [Fig. 3(a)]. A power-law fit of the form $\Omega_N = \Omega N^\alpha$ yields an exponent of $\alpha = 0.49(10)$. Deviations toward higher Rabi frequencies for small N might be due to a residual detuning of the coupling lasers that we calibrate via spectroscopy on a dilute atomic cloud with an uncertainty of ± 200 kHz. A systematic lower Rabi frequency at large N can be caused by a residual inhomogeneity of the laser coupling (up to 10%) due to its Gaussian intensity profile. Also, the observed onset of a breakdown of the blockade for our largest prepared samples results in a deviation from the $\sqrt{N}$ scaling. The latter effect is additionally visible in the extracted steady-state mean Rydberg atom number ηA. For all but the largest sample size, we find $A = 0.51(2)$, consistent with the expected value of 0.5. For $N = 185$, it increases significantly to $A = 0.65(12)$. To answer the question whether the collective speedup can be exploited for quantum operations or whether decoherence effects dominate, we analyze the quality factor of the Rabi oscillations, which is given by the product of the decay time τ of the measured oscillations and the Rabi frequency

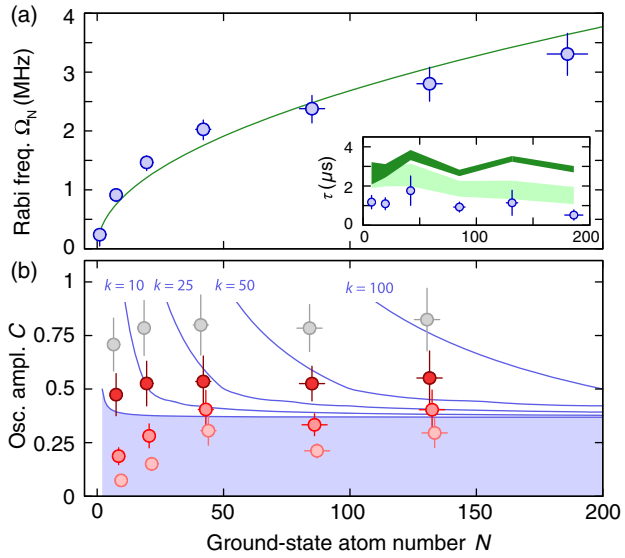

FIG. 3. Scaling of the Rabi frequency and entanglement. (a) Extracted values of Ω_N (blue points) versus average initial atom number N for the data shown in Figs. 1(d) and 2 with a power-law fit (green line). The inset shows the exponential decay time of the Rabi oscillations (blue points). The expected decay based on the reference sample atom-number fluctuations (dark green shading) and additionally taking into account noise in the pulse area (light green shading) are shown for comparison. (b) Extracted oscillation amplitude C of the collective Rabi oscillation versus atom number N after one, three, and five half cycles of oscillation (red data points with increasing lightness, shifted slightly horizontally for better visibility). The gray points show the oscillation amplitude after one half cycle corrected for the measured detection efficiency. The blue shaded area bounded by the lowest blue line includes all classical states with fully separable density matrices. Different bounds for k-particle separability are additionally shown by the blue lines. Error bars in (a) take experimental day-to-day variations of the single-atom Rabi frequency Ω (10%) and the detuning (± 200 kHz) into account. All error bars in (b) are 1σ statistical uncertainty from the fits.

Ω_N. Indeed, we find a peaking quality factor for $N = 131$ due to the increasing oscillation frequency but constant decay time $\tau \approx 1$ μs in the fully blockaded regime [inset of Fig. 3(a)]. Among the limiting factors for the coherence time are residual atom number and coupling power fluctuations [8(2)%]. However, these alone cannot explain the observed decay [inset of Fig. 3(a)]. For small atom numbers, additional decoherence might be due to phase noise and slow frequency drifts of the lasers, while the inhomogeneity in the Rabi coupling becomes significant at larger N. Additionally, weak coupling to pair potentials involving nearby Rydberg states would result in an approximately size-independent decoherence mechanism that might contribute to the observed dephasing [9].

Next to the collective enhancement of the optical coupling, the structure of the excited state itself bears the marks of the strong particle correlations. The unambiguous proof that the experimentally prepared excited state of the superatom $|\tilde{W}\rangle$ is indeed the N-particle entangled W state would require full state tomography [39], which is not feasible in our setup. However, we will show that under few plausible assumptions, the experimental observations are incompatible with the expectations for a fully separable state. To this end, we follow the ideas developed in Ref. [8] to detect entanglement between the atoms described by the many-body state $|\tilde{W}\rangle$ via the overlap $\alpha = |\langle W|\tilde{W}\rangle|^2$ with the W state. The overlap α of any fully separable N-atom state $|\Phi\rangle = |\phi_1\rangle \otimes \ldots \otimes |\phi_N\rangle$, where $|\phi_i\rangle$ describes the state of the ith two-level atom, is bounded by $\alpha_{\max}$ (approximately 0.37 for large N), such that $\alpha > \alpha_{\max}$ necessarily requires entanglement. Furthermore, for any k-atom inseparable (entangled) state, there is a maximum overlap $\alpha_{\max}^{(k)}$, which enables us to infer the minimum number of entangled particles k from a given α. Especially, the minimum fraction of entangled particles k/N is directly given by α if $\alpha > 0.5$. The preceding discussion can be generalized to the experimentally relevant mixed states using the density-matrix formalism [8].

The remaining challenge to extract α from the experimental data requires three conditions to be met. These are, first, maximally one Rydberg excitation in the system; second, the absence of shot-to-shot fluctuating relative phases in the sample; and, third, symmetric coupling to the Rydberg state. The first condition, which especially prohibits the use of any postselection of the experimental data, is well met for all but the largest superatoms. Also, the second requirement is fulfilled, since motional dephasing is absent due to the localization of each atom in the Mott insulating state in the optical lattice. Furthermore, the extension of the two-dimensional system in the direction of the excitation light wave vector $\mathbf{k}$ is vanishing such that there is no spin wave [40] present and $\mathbf{k} \cdot (\mathbf{r_i} - \mathbf{r_j}) = 0$ for any two atoms i, j located at $\mathbf{r_i}$ and $\mathbf{r_j}$. The third and last condition is also fulfilled given that effects due to the small coupling inhomogeneity of our lasers are negligible on the experimentally investigated time scale. In the subspace of zero and one excitation, the spatially uniform Rabi driving couples only the symmetric states $|0\rangle$ and $|W\rangle$. Population in any of the $N - 1$ orthogonal states shows no dynamics in that subspace but leads to a reduction of the oscillation amplitude $C(t)$ of the Rabi oscillations. Hence, $C(t)$ gives a lower bound for the overlap $\alpha(t)$ [41]. We extract $C(t) = \eta e^{-t/\tau}$ from the fitted exponentially decaying envelope of the Rabi oscillation data.

In Fig. 3(b), we show that $C(t)$ at the Rabi oscillation maximum after the first half Rabi cycle is above the threshold for entanglement for all superatom sizes that fulfil the above-mentioned criteria, even without correcting for the detection efficiency η. For longer times, $C(t)$ decays into the classically allowed region. We exclude the $N = 185$ superatom from the analysis due to the small

yet finite population of the $n_e = 2$ subspace. Removing the known systematic effect due to the finite detection efficiency η, we obtain a lower bound for the average W-state overlap of $\alpha = 0.78(17)$ at the first maximum. The bounds in Fig. 3(b) show that our data suggest an inseparable block size of approximately 100 atoms for the $N = 131$ superatom.

To investigate the coherence of the collective qubit further, we use a $N = 38(3)$ atom ensemble for Ramsey interferometry [9,26,27,42]. First, we prepare a coherent superposition of $|0\rangle$ and $|\tilde{W}\rangle$ by a $\pi/2$ pulse of length $T = \pi/(2\Omega\sqrt{N})$. After a variable hold time T_R, a second $\pi/2$ pulse is applied and the mean Rydberg atom number N_e is measured (Fig. 4). Due to the ac Stark shift created by the red 780 nm-laser during the excitation pulse, the calibrated transition frequency differs from the bare ground to Rydberg state transition frequency, which defines the reference for the Ramsey interferometer. Therefore, the observed phase accumulation rate is given by this ac Stark shift and agrees well with an independent calibration of the latter via microwave spectroscopy. In contrast to the Rabi measurements, the coupling light is switched off here during most of the sequence, such that decoherence mechanisms induced by the laser coupling are absent. Indeed, we find that the extracted decay time of the Ramsey fringe of $\tau_R = 2.2(4)$ μs exceeds the damping τ of the Rabi oscillations. We also perform Ramsey interferometry for different superatom sizes N and find within experimental uncertainty τ_R approximately independent of N. These results imply that laser phase fluctuations and local single-particle dephasing are not limiting for the Rabi contrast, indicating that either we underestimate the influence of our laser power fluctuations or interaction effects beyond the simple blockade picture are present.

When increasing the sample to a size where the maximum distance between two atoms D approaches the blockade radius, the isolated superatom picture is expected to gradually break down [34,43]. The gap to doubly excited states with two atoms pinned to the diagonal corners of the prepared square-shaped density distribution is smallest, such that these are the first doubly excited states populated. We discussed already several indications of this blockade breakdown for the $N = 185$ atom sample. Here, the maximum separation of two atoms is $D = 9.8(7)$ μm, close to the blockade radius $R_b = 11.7$ μm. Even though comparing these two length scales suggests a fully blockaded ensemble, we start to observe—with low probability—the coupling to multiply excited states as expected from calculations in a reduced Hilbert space [29]. In Fig. 5, we study the effects of the doubly excited states on the decay of the Rabi oscillation for this setting by postselecting the acquired data to single and double Rydberg events. The decay time of the singly excited component is 2 times larger compared to the full sample and agrees with the prediction of the numerical calculation. This shows that the observed decay is significantly influenced by the dephasing due to double excitation. We observe a slow increase of the doubly excited fraction (also in agreement with theory) that is consistent with the picture of two interacting excitations [44]. Their interaction energy corresponds to the energy shift Δ_{vdW} at the distance D, resulting in a detuned optical coupling. At the same time, the collective enhancement of the coupling to this state is only $\sqrt{2}$ reflecting the two

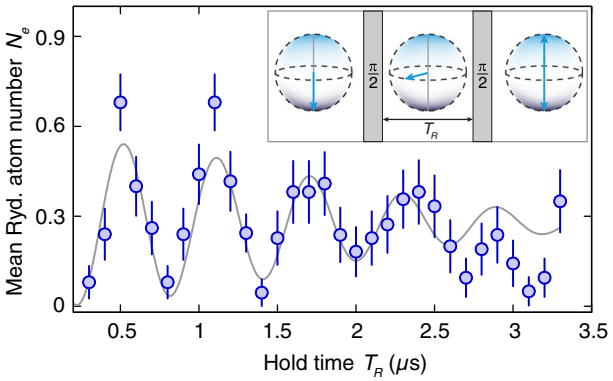

FIG. 4. Superatom Ramsey spectroscopy. Evolution of the mean Rydberg atom number N_e (blue points) versus hold time T_R between the two $\pi/2$ pulses (schematic in the inset) and sinusoidal fit with Gaussian decay (gray line) for an initial sample size of $N = 38(3)$ atoms. All error bars are s.e.m.

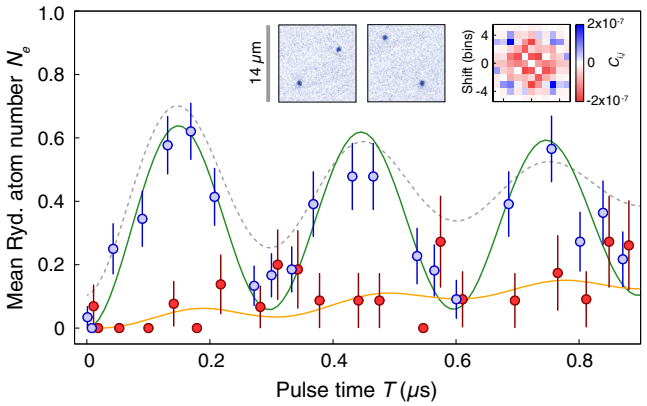

FIG. 5. Breakdown of the blockade. Measurement of the collective Rabi oscillation in a sample with $N = 185(8)$ atoms. (a) The contribution of states with $n_e = 1$ (blue points) and $n_e = 2$ (red points, shifted slightly horizontally for better visibility) agrees with the theoretical calculation (green and orange solid lines, scaled by extracted detection efficiency η). For comparison, we show the fit (gray line) to the mean (see Fig. 2), which shows twice faster dephasing than the $n_e = 1$ subspace alone. We have chosen the simplest possible fitting model with a constant offset such that the increasing fraction of double excitation results in a upward shift of the fit for small times. The inset shows two exemplary single shots with $n_e = 2$ (field of view 14×14 μm^2, indicated by gray bar) and the two-dimensional pair-correlation function $C_{i,j}$ of all $n_e = 2$ events. Color scale: red (anticorrelation) to blue (correlation). Data binned 4×4 sites. All error bars are s.e.m.

possible orientations along the diagonals. The resulting time scale $\pi/\sqrt{2\Omega^2+\Delta_{\mathrm{vdW}}^2}$ matches roughly the observed slow rise of the doubly excited states; however, explaining their probability quantitatively requires a more complex model including also atoms close to the corners of the square. Spatial correlation measurements confirm the localization of the doubly excited events at the diagonal corners (inset of Fig. 5). Low statistics requires here the binning of 4×4 lattice sites for the evaluation of the two-point correlation $C_{i,j}=\langle\langle P_{(x,y)}P_{(x+i,y+j)}\rangle-\langle P_{(x,y)}\rangle\langle P_{(x+i,y+j)}\rangle\rangle_{x,y}$. Here, $P_{(i,j)}$ is the probability of finding a Rydberg excitation in bin (i,j) and $\langle\cdot\rangle_{x,y}$ and $\langle\cdot\rangle$ denote the spatial and ensemble averages.

In conclusion, we demonstrated coherent control and 2 orders of magnitude scalability of Rydberg superatoms. Using *in situ* microscopical detection of the Rydberg atoms, we confirmed the superatom picture and inferred the W-state overlap and the presence of entanglement in the involved singly excited many-body states. We also demonstrated that the collectively enhanced coupling can be harnessed to increase the fidelity of collective qubit rotations under realistic experimental conditions. The experiments confirmed that coupling to many-body states with larger Rydberg occupation leads to interaction-induced dephasing, strongly supporting the coherent description of our previous experiment on short time scales [29,38]. Together with earlier works [10,11,32], our results pave the way toward the controlled stepwise preparation of higher Dicke states [4], which have been proposed for metrology at the Heisenberg limit [45], and they promise to shed light on macroscopic entangled quantum systems [46].

We thank Marc Cheneau and Takeshi Fukuhara for valuable discussions and Jae-yoon Choi for proofreading the manuscript. T. M. thanks the International Institute of Physics (Brazil) for the hospitality during the completion of the paper. We acknowledge funding by MPG, EU (UQUAM, SIQS), and the Körber Foundation.

[1] P. Münstermann, T. Fischer, P. Maunz, P. W. H. Pinkse, and G. Rempe, *Observation of Cavity-Mediated Long-Range Light Forces between Strongly Coupled Atoms*, Phys. Rev. Lett. **84**, 4068 (2000).

[2] M. Saffman, T. G. Walker, and K. Mølmer, *Quantum Information with Rydberg Atoms*, Rev. Mod. Phys. **82**, 2313 (2010).

[3] D. Jaksch, J. I. Cirac, P. Zoller, S. L. Rolston, R. Côté, and M. D. Lukin, *Fast Quantum Gates for Neutral Atoms*, Phys. Rev. Lett. **85**, 2208 (2000).

[4] M. D. Lukin, M. Fleischhauer, R. Cote, L. M. Duan, D. Jaksch, J. I. Cirac, and P. Zoller, *Dipole Blockade and Quantum Information Processing in Mesoscopic Atomic Ensembles*, Phys. Rev. Lett. **87**, 037901 (2001).

[5] E. Urban, T. A. Johnson, T. Henage, L. Isenhower, D. D. Yavuz, T. G. Walker, and M. Saffman, *Observation of Rydberg Blockade between Two Atoms*, Nat. Phys. **5**, 110 (2009).

[6] A. Gaëtan, Y. Miroshnychenko, T. Wilk, A. Chotia, M. Viteau, D. Comparat, P. Pillet, A. Browaeys, and P. Grangier, *Observation of Collective Excitation of Two Individual Atoms in the Rydberg Blockade Regime*, Nat. Phys. **5**, 115 (2009).

[7] R. H. Dicke, *Coherence in Spontaneous Radiation Processes*, Phys. Rev. **93**, 99 (1954).

[8] F. Haas, J. Volz, R. Gehr, J. Reichel, and J. Estève, *Entangled States of More Than 40 Atoms in an Optical Fiber Cavity*, Science **344**, 180 (2014).

[9] M. Ebert, M. Kwon, T. G. Walker, and M. Saffman, arXiv:1501.04083.

[10] L. Isenhower, E. Urban, X. L. Zhang, A. T. Gill, T. Henage, T. A. Johnson, T. G. Walker, and M. Saffman, *Demonstration of a Neutral Atom Controlled-NOT Quantum Gate*, Phys. Rev. Lett. **104**, 010503 (2010).

[11] T. Wilk, A. Gaëtan, C. Evellin, J. Wolters, Y. Miroshnychenko, P. Grangier, and A. Browaeys, *Entanglement of Two Individual Neutral Atoms Using Rydberg Blockade*, Phys. Rev. Lett. **104**, 010502 (2010).

[12] Y.-Y. Jau, A. M. Hankin, T. Keating, I. H. Deutsch, and G. W. Biedermann, arXiv:1501.03862.

[13] M. Saffman and T. G. Walker, *Entangling Single- and N-Atom Qubits for Fast Quantum State Detection and Transmission*, Phys. Rev. A **72**, 042302 (2005).

[14] L. H. Pedersen and K. Mølmer, *Few Qubit Atom-Light Interfaces with Collective Encoding*, Phys. Rev. A **79**, 012320 (2009).

[15] L. Li, Y. O. Dudin, and A. Kuzmich, *Entanglement between Light and an Optical Atomic Excitation*, Nature (London) **498**, 466 (2013).

[16] W. Dür, G. Vidal, and J. I. Cirac, *Three Qubits Can Be Entangled in Two Inequivalent Ways*, Phys. Rev. A **62**, 062314 (2000).

[17] E. Brion, L. H. Pedersen, M. Saffman, and K. Mølmer, *Error Correction in Ensemble Registers for Quantum Repeaters and Quantum Computers*, Phys. Rev. Lett. **100**, 110506 (2008).

[18] E. Brion, K. Mølmer, and M. Saffman, *Quantum Computing with Collective Ensembles of Multilevel Systems*, Phys. Rev. Lett. **99**, 260501 (2007).

[19] M. Saffman and K. Mølmer, *Scaling the Neutral-Atom Rydberg Gate Quantum Computer by Collective Encoding in Holmium Atoms*, Phys. Rev. A **78**, 012336 (2008).

[20] M. Müller, I. Lesanovsky, H. Weimer, H. P. Büchler, and P. Zoller, *Mesoscopic Rydberg Gate Based on Electromagnetically Induced Transparency*, Phys. Rev. Lett. **102**, 170502 (2009).

[21] L. Isenhower, M. Saffman, and K. Mølmer, *Multibit C_kNOT Quantum Gates via Rydberg Blockade*, Quantum Inf. Process. **10**, 755 (2011).

[22] J. Deiglmayr, M. Reetz-Lamour, T. Amthor, S. Westermann, A. L. de Oliveira, and M. Weidemüller, *Coherent Excitation of Rydberg Atoms in an Ultracold Gas*, Opt. Commun. **264**, 293 (2006).

[23] R. Heidemann, U. Raitzsch, V. Bendkowsky, B. Butscher, R. Löw, L. Santos, and T. Pfau, *Evidence for Coherent Collective Rydberg Excitation in the Strong Blockade Regime*, Phys. Rev. Lett. **99**, 163601 (2007).

[24] T. A. Johnson, E. Urban, T. Henage, L. Isenhower, D. D. Yavuz, T. G. Walker, and M. Saffman, *Rabi Oscillations between Ground and Rydberg States with Dipole-Dipole Atomic Interactions*, Phys. Rev. Lett. **100**, 113003 (2008).

[25] M. Reetz-Lamour, T. Amthor, J. Deiglmayr, and M. Weidemüller, *Rabi Oscillations and Excitation Trapping in the Coherent Excitation of a Mesoscopic Frozen Rydberg Gas*, Phys. Rev. Lett. **100**, 253001 (2008).

[26] U. Raitzsch, V. Bendkowsky, R. Heidemann, B. Butscher, R. Löw, and T. Pfau, *Echo Experiments in a Strongly Interacting Rydberg Gas*, Phys. Rev. Lett. **100**, 013002 (2008).

[27] K. C. Younge and G. Raithel, *Rotary Echo Tests of Coherence in Rydberg-Atom Excitation*, New J. Phys. **11**, 043006 (2009).

[28] M. Viteau, M. G. Bason, J. Radogostowicz, N. Malossi, D. Ciampini, O. Morsch, and E. Arimondo, *Rydberg Excitations in Bose-Einstein Condensates in Quasi-One-Dimensional Potentials and Optical Lattices*, Phys. Rev. Lett. **107**, 060402 (2011).

[29] P. Schauß, M. Cheneau, M. Endres, T. Fukuhara, S. Hild, A. Omran, T. Pohl, C. Gross, S. Kuhr, and I. Bloch, *Observation of Spatially Ordered Structures in a Two-Dimensional Rydberg Gas*, Nature (London) **491**, 87 (2012).

[30] A. M. Hankin, Y.-Y. Jau, L. P. Parazzoli, C. W. Chou, D. J. Armstrong, A. J. Landahl, and G. W. Biedermann, *Two-Atom Rydberg Blockade Using Direct 6S to nP Excitation*, Phys. Rev. A **89**, 033416 (2014).

[31] D. Barredo, S. Ravets, H. Labuhn, L. Béguin, A. Vernier, F. Nogrette, T. Lahaye, and A. Browaeys, *Demonstration of a Strong Rydberg Blockade in Three-Atom Systems with Anisotropic Interactions*, Phys. Rev. Lett. **112**, 183002 (2014).

[32] M. Ebert, A. Gill, M. Gibbons, X. Zhang, M. Saffman, and T. G. Walker, *Atomic Fock State Preparation Using Rydberg Blockade*, Phys. Rev. Lett. **112**, 043602 (2014).

[33] Y. O. Dudin, L. Li, F. Bariani, and A. Kuzmich, *Observation of Coherent Many-Body Rabi Oscillations*, Nat. Phys. **8**, 790 (2012).

[34] T. M. Weber, M. Höning, T. Niederprüm, T. Manthey, O. Thomas, V. Guarrera, M. Fleischhauer, G. Barontini, and H. Ott, *Mesoscopic Rydberg-Blockaded Ensembles in the Superatom Regime and Beyond*, Nat. Phys. **11**, 157 (2015).

[35] C. T. Lee, *Q Representation of the Atomic Coherent States and the Origin of Fluctuations in Superfluorescence*, Phys. Rev. A **30**, 3308 (1984).

[36] F. T. Arecchi, E. Courtens, R. Gilmore, and H. Thomas, *Atomic Coherent States in Quantum Optics*, Phys. Rev. A **6**, 2211 (1972).

[37] C. Weitenberg, M. Endres, J. F. Sherson, M. Cheneau, P. Schauß, T. Fukuhara, I. Bloch, and S. Kuhr, *Single-Spin Addressing in an Atomic Mott Insulator*, Nature (London) **471**, 319 (2011).

[38] P. Schauß, J. Zeiher, T. Fukuhara, S. Hild, M. Cheneau, T. Macrì, T. Pohl, I. Bloch, and C. Gross, *Crystallization in Ising Quantum Magnets*, Science **347**, 1455 (2015).

[39] H. Häffner, W. Hänsel, C. F. Roos, J. Benhelm, D. Chek-al-kar, M. Chwalla, T. Körber, U. D. Rapol, M. Riebe, P. O. Schmidt, C. Becher, O. Gühne, W. Dür, and R. Blatt, *Scalable Multiparticle Entanglement of Trapped Ions*, Nature (London) **438**, 643 (2005).

[40] Y. O. Dudin and A. Kuzmich, *Strongly Interacting Rydberg Excitations of a Cold Atomic Gas*, Science **336**, 887 (2012).

[41] See Supplemental Material at http://link.aps.org/supplemental/10.1103/PhysRevX.5.031015 for a more detailed explanation of the extraction of the W state overlap from the Rabi oscillation amplitude.

[42] J. Nipper, J. B. Balewski, A. T. Krupp, B. Butscher, R. Löw, and T. Pfau, *Highly Resolved Measurements of Stark-Tuned Förster Resonances between Rydberg Atoms*, Phys. Rev. Lett. **108**, 113001 (2012).

[43] I. I. Ryabtsev, D. B. Tretyakov, I. I. Beterov, V. M. Entin, and E. A. Yakshina, *Stark-Tuned Förster Resonance and Dipole Blockade for Two to Five Cold Rydberg Atoms: Monte Carlo Simulations for Various Spatial Configurations*, Phys. Rev. A **82**, 053409 (2010).

[44] J. Stanojevic and R. Côté, *Many-Body Rabi Oscillations of Rydberg Excitation in Small Mesoscopic Samples*, Phys. Rev. A **80**, 033418 (2009).

[45] M. J. Holland and K. Burnett, *Interferometric Detection of Optical Phase Shifts at the Heisenberg Limit*, Phys. Rev. Lett. **71**, 1355 (1993).

[46] T. Opatrný and K. Mølmer, *Spin Squeezing and Schrödinger-Cat-State Generation in Atomic Samples with Rydberg Blockade*, Phys. Rev. A **86**, 023845 (2012).